

Coverage dependence of the microscopic diffusion of Na atoms on the Cu(001) surface: A combined helium atom scattering experiment and molecular dynamics study

J. Ellis,¹ A. P. Graham,² F. Hofmann,² and J. P. Toennies²

¹*Cavendish Laboratory, Madingley Road, Cambridge CB3 0HE, United Kingdom*

²*Max-Planck-Institut für Strömungsforschung, Bunsenstrasse 10, 37073 Göttingen, Germany*

(Received 18 October 2000; published 20 April 2001)

Previous quasielastic helium atom scattering studies of the low-coverage diffusion of sodium ($\Theta_{\text{Na}} \leq 0.05$) on the Cu(001) surface have been extended up to coverages of $\Theta_{\text{Na}} = 0.18$. These measurements, at surface temperatures between $T_s = 180$ and 390 K and parallel wave vector transfers up to $\Delta K = 3.34 \text{ \AA}^{-1}$, are compared with molecular dynamics simulations that include the dipole-dipole interactions between the Na atoms. Whereas the simulations can explain the increase in the observed activation energy and the change in the shape of the peak width with momentum transfer, they fail to reproduce the marked overall increases in peak widths observed as the coverage is increased. Several possible explanations are discussed and are shown to be unable to explain the results.

DOI: 10.1103/PhysRevB.63.195408

PACS number(s): 68.35.Fx, 68.35.Ja, 34.20.Cf, 05.10.Gg

I. INTRODUCTION

The diffusion of adsorbates on single-crystal surfaces is an important elementary microscopic step governing the dynamics of many processes occurring at surfaces such as chemical reactions (catalysis) and epitaxial growth.¹ A large range of experimental techniques have been developed over the years for the study of diffusion at surfaces.¹ Of these the method of field ion microscopy² (FIM) provides perhaps the most detailed information on the elementary microscopic processes, but is limited largely to refractory metal atoms on a refractory metal surface. Recently, several other techniques such as laser-induced desorption (LID),³ linear optical diffraction,⁴ second-harmonic generation (SHG),^{5,6} scanning tunneling microscopy (STM),⁷ and quasielastic helium atom scattering (QHAS),⁸ which is the surface analog of quasielastic neutron scattering,⁹ have been successfully implemented. Experimental methods such as LID and SHG are sensitive to adsorbate diffusion over length scales of the order of several micrometers and are therefore sensitive to the chemical diffusion coefficient. In the microscopic techniques FIM and STM, snapshots are made at successive times of the actual positions of the atoms on the surface. The other microscopic technique, QHAS, is sensitive only to the actual motion of the individual adsorbates. At present the QHAS technique is limited by the instrumental resolution to fast diffusion with a diffusion coefficient $D \geq 10^{-6} \text{ cm}^2/\text{sec}$,¹⁰⁻¹⁵ whereas STM and FIM are restricted to slow diffusion with $D \leq 10^{-14} \text{ cm}^2/\text{sec}$.⁷

Previously, the QHAS method has been applied to more than five different metal/metal and nine adsorbate/metal systems.^{14,15} Of these, the diffusion of sodium adatoms on the Cu(001) surface has been the most extensively studied.^{13,16-18} In the most recent investigation both the quasielastic peak broadening and the frustrated translational vibration mode were studied over a wide range of temperatures (150–390 K) and wave vector transfers for both Cu(001) azimuthal high-symmetry directions.¹⁶ Since this study was restricted to low coverages, $\Theta_{\text{Na}} < 0.05$ monolayer

[$\Theta_{\text{Na}} = 1$ corresponds to one sodium atom per Cu(001) substrate atom or $n = 1.53 \times 10^{19} \text{ atoms/cm}^2$] the interaction between sodium atoms could be safely neglected and the results were compared with a full simulation based on the Langevin equations for single sodium atoms with a friction coefficient to account for the dynamical coupling to substrate degrees of freedom. From the best fit of all the data a detailed potential energy surface governing the lateral motion of the individual atoms was determined.¹⁶

In the present study these experiments have been extended to higher coverages up to $\Theta_{\text{Na}} = 0.18$ where it is known from a companion structural study¹⁹ at $T_s = 50 \text{ K}$ that there are strong repulsive interactions between the sodium atoms which lead to well-defined adsorbate lattices.

Other inelastic helium atom scattering²⁰ experiments have also shown an effect of the Na-Na interaction on the frustrated translation mode (T mode) at the coverages studied here. To establish the role of the direct dipole-dipole repulsion interactions the present QHAS diffusion experiments are compared with detailed molecular dynamics (MD) simulations based on the Langevin dynamics method. These extensive comparisons show that many of the features of the experiment can be well reproduced by introduction of the dipole-dipole repulsion, which was calculated by Lau and Kohn²¹ to be twice the repulsion between two free dipoles, where the sodium dipole moment is determined from work function measurements.^{22,23} With increasing coverage, however, the experimental QHAS peak widths are found to become increasingly larger than predicted. By changing the strength of the adsorbate-adsorbate interaction it is not possible to explain both the absolute magnitude of the observed widths and the other experimental features. Other possible explanations for this discrepancy are also examined, and are not able to explain the differences.

Recently Cucchetti and Ying²³ reported a comparison based on a similar theory with some of the experimental data reported here. The present publication contains a final analysis of the full set of experimental data, which differ in some respects from those presented in Ref. 23. Moreover, it ad-

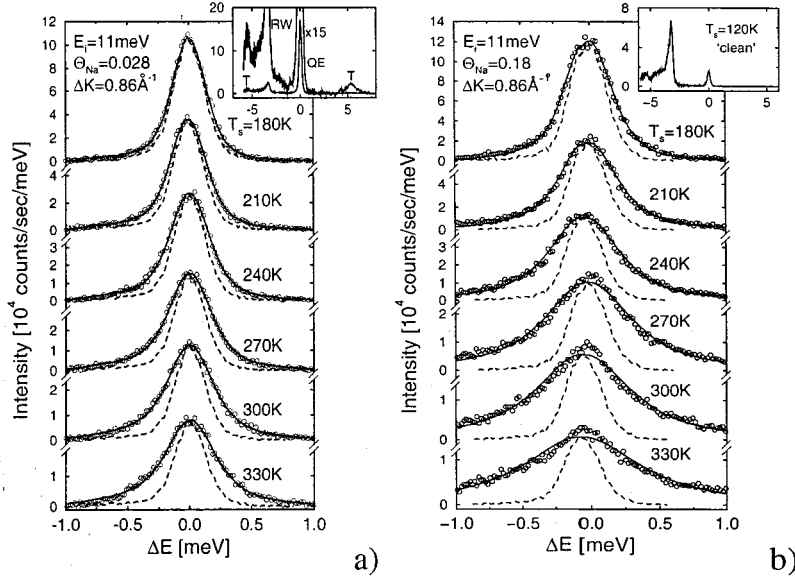


FIG. 1. A series of inelastic helium scattering TOF spectra in the vicinity of the QE peak converted to an energy transfer scale for various temperatures of a Cu(001) surface with $\Theta_{\text{Na}} =$ (a) 0.028 and (b) 0.18 adsorbed sodium. The inset to (a) shows an extended TOF spectrum for a temperature of $T_s = 180$ K with the inelastic peaks from the parallel frustrated translational mode (T) and the surface Rayleigh wave (RW). The inset to (b) shows an extended TOF spectrum for the clean surface. The TOF spectra were obtained with an 11.2 meV helium beam scattered in the $[100]$ surface direction with a wave vector transfer of $\Delta K = 0.68 \text{ \AA}^{-1}$. The open circles show the experimental data points, while the dashed lines show the response function of the helium scattering apparatus under the same conditions. The solid line through the data points is a convolution of the instrument response function with a best-fit Lorentzian peak shape, which is used to extract the quasielastic broadening of the peak.

dresses the important issue of why the measured ΔK dependence of the QHAS peak widths is significantly larger than in the theoretical simulations.

The paper is organized in the following way. In Sec. II the experimental details are described, followed, in Sec. III, by the QHAS experimental results. In Sec. IV the details of the MD simulations are discussed and subsequently a comparison between the experimental and MD results is made in Sec. V. In Sec. VI the results are discussed and the paper closes with a summary of the main conclusions in Sec. VII.

II. EXPERIMENTAL PROCEDURE

The HUGO II high-resolution helium atom scattering apparatus^{24,25} used here has a supersonic atomic helium beam source of $\Delta v/v \sim 1\%$ and a time-of-flight arm of 1.4 m length at a fixed angle of $\theta_{\text{SD}} = 95.8^\circ$ to the incident beam. The parallel wave vector transfer (ΔK) at the crystal was varied by changing the incident angle of the beam to the surface and for elastic scattering is given by

$$\Delta K = k_i [\sin(\theta_{\text{SD}} - \theta_i) - \sin(\theta_i)]. \quad (1)$$

The energy resolution at the beam energy used in the present experiments ($E_i = 11.2$ meV) was $\Delta E_i = 0.30$ meV. The angular resolution is typically $\Delta \theta = 0.3^\circ$ which, at an incident energy of $E_i = 11.2$ meV, corresponds to a parallel wave vector transfer resolution of $\delta(\Delta K) \approx 0.03 \text{ \AA}^{-1}$. The Cu(001) single-crystal surface was cut and mechanically polished to an accuracy of better than 0.25° . The copper sample was then cleaned in ultrahigh vacuum with repeated cycles of

sputtering and annealing until no contamination could be detected with Auger spectroscopy ($<1\%$) and elastic and inelastic helium scattering showed a smooth surface with a high degree of order.

Sodium was evaporated from a SAES Getters alkali-metal source,²⁶ directed normal to the surface and the coverage Θ_{Na} was monitored by measuring the attenuation of the specular helium peak²⁷ with an estimated error in the coverage of $\delta\Theta_{\text{Na}} \approx 0.005$. The surface temperature was measured using a Ni-CrNi (K -type) thermocouple attached to the side of the copper sample with an accuracy estimated to be $\delta T_s \sim \pm 5$ K. The base pressure (i.e., excluding the partial pressure of helium from the beam) was less than 2×10^{-11} mbar. The specular intensity from the sodium-covered surface changed by less than 10% over a period of 2 h, after which the surface was cleaned and a fresh layer of sodium deposited.

III. RESULTS

Figure 1(a) shows a typical series of measured time-of-flight (TOF) spectra of the quasielastic (QE) peak, converted to an energy transfer scale (ΔE), for six different surface temperatures between $T_s = 180$ and 330 K, along the $[100]$ azimuth, and a low sodium coverage of $\Theta_{\text{Na}} = 0.028$. The incident beam energy was 11.2 meV and the incident angle was $\theta_i = 39.9^\circ$ corresponding to a fixed parallel wave vector transfer of $\Delta K = 0.86 \text{ \AA}^{-1}$. The inset illustrates a complete TOF spectrum in which, in addition to the QE peak, the inelastic structures due to the sodium frustrated translation

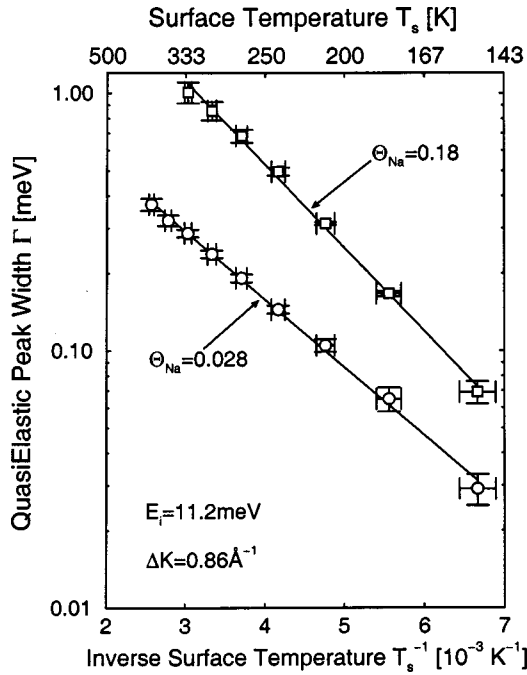


FIG. 2. Arrhenius plots of the quasielastic peak widths (Γ) versus inverse surface temperature (T_s) for sodium coverages of $\Theta_{\text{Na}} = 0.028$ and 0.18 for a parallel wave vector transfer of $\Delta K = 0.86 \text{ \AA}^{-1}$. The beam energy in both measurements was 11.2 meV along the $[100]$ direction. The least-squares fit of the data points yields effective activation energies of $E_{\text{act}} = 53.2 \pm 0.9 \text{ meV}$ for $\Theta_{\text{Na}} = 0.028$ and $E_{\text{act}} = 63.9 \pm 1.8 \text{ meV}$ for $\Theta_{\text{Na}} = 0.18$.

mode (T mode) and the substrate surface Rayleigh wave are also apparent. These inelastic peaks have been extensively analyzed and the results are reported in Refs. 16, 18, and 28. The dashed lines in each spectrum in Figs. 1(a) and 1(b) show the experimental energy resolution function. The difference between the measured TOF distribution and the dashed line is attributed to quasielastic broadening, which in Fig. 1 is seen to increase significantly with increasing surface temperature. These results are in excellent agreement with earlier measurements under nearly the same conditions.¹³ For comparison Fig. 1(b) shows a series of typical spectra for a factor of 6 greater coverage, $\Theta_{\text{Na}} = 0.18$, under otherwise identical conditions as in Fig. 1(a). Compared to the low-coverage data, a much greater QE broadening is found at the higher coverage.

The quasielastic peak width was extracted by a least-squares fitting of a convolution of the instrument response and the theoretically expected Lorentz function to each TOF spectrum.^{14,29} The results of the fitting procedure are shown by the solid lines for each spectrum. As can be seen, the overall fit is well within the experimental scatter in the data points. The extracted Lorentz peak energy full widths at half maximum (FWHM) Γ from the TOF series shown in Figs. 1(a) and 1(b) are plotted in Fig. 2 on a logarithmic scale versus the inverse surface temperature T_s . The peak width errors were estimated from a significant number (~ 50) of trial fits to simulated TOF spectra generated with the same noise level and peak width as each of the measured TOF spectra.¹⁴ The resulting error calculated for a typical TOF

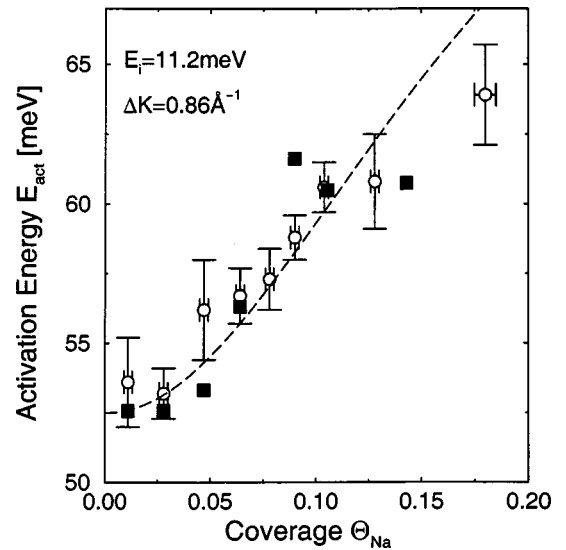


FIG. 3. The effective activation energy E_{act} measured for a parallel wave vector of $\Delta K = 0.86 \text{ \AA}^{-1}$ as a function of sodium coverage (open circles with error bars). The filled squares show the effective barrier calculated from the molecular dynamics simulations for the same value of ΔK . The dashed line shows the variation in activation energy calculated directly from the Lau and Kohn adatom-adatom dipole-dipole interaction model discussed in Sec. V C.

spectrum with a constant background count rate of 50 counts/channel and a peak of 1000 counts/channel at maximum and $\Gamma = 0.100 \text{ meV}$ width was determined to be $\delta\Gamma \approx 0.005 \text{ meV}$ using this procedure.¹⁴ From the slope of the data points an effective activation energy E_{act} was extracted. Figure 3 shows the values of E_{act} obtained in this way for a range of sodium coverages and a parallel wave vector transfer of $\Delta K = 0.86 \text{ \AA}^{-1}$.

Figure 4(a) shows a series of TOF spectra for different values of the parallel wave vector along the $[100]$ azimuth all at a low sodium coverage of $\Theta_{\text{Na}} = 0.028$ and a surface temperature of $T_s = 300 \text{ K}$. The peak width is observed to increase significantly to a maximum at $\Delta K = 1.74 \text{ \AA}^{-1}$ before decreasing to a minimum at $\Delta K = 3.34 \text{ \AA}^{-1}$, close to the first diffraction peak position for the Cu(001) surface in the $[100]$ direction ($\Delta K = G = 3.48 \text{ \AA}^{-1}$). Over the same range of ΔK the quasielastic peak intensity falls by nearly four orders of magnitude. In Fig. 4(b) a series of TOF spectra are shown for a higher sodium coverage of $\Theta_{\text{Na}} = 0.106$ under the same scattering conditions and also for a surface temperature of $T_s = 300 \text{ K}$. For this higher coverage the quasielastic peak is much broader for low values of parallel wave vector, with a smaller increase in width toward $\Delta K = 1.74 \text{ \AA}^{-1}$ than for $\Theta_{\text{Na}} = 0.028$. In addition, the quasielastic peak is broadened appreciably at $\Delta K = 3.34 \text{ \AA}^{-1}$, near the diffraction peak, compared to the relatively small broadening observed for a coverage of $\Theta_{\text{Na}} = 0.028$ in Fig. 4(a). The quasielastic peak is observed to be consistently broader for $\Theta_{\text{Na}} = 0.106$ than for $\Theta_{\text{Na}} = 0.028$.

IV. MOLECULAR DYNAMICS SIMULATIONS

To assist in interpretation of the QHAS data, a molecular dynamics simulation of the diffusion of sodium on Cu(100)

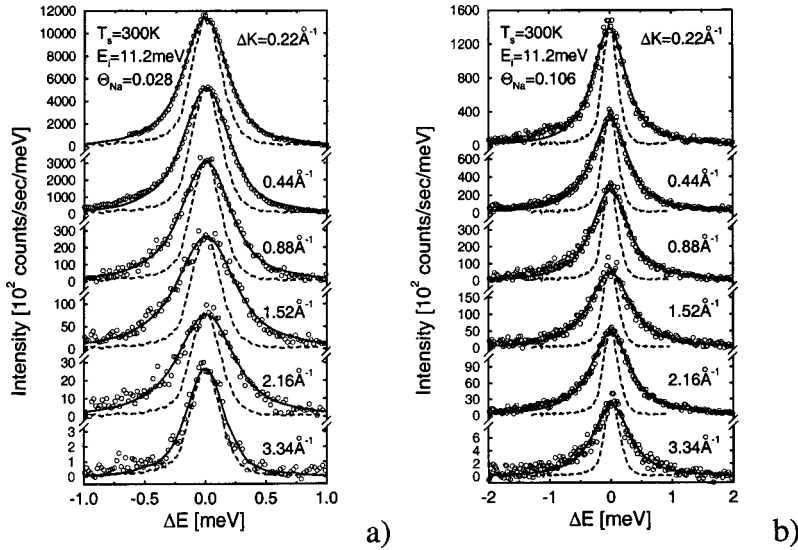


FIG. 4. A series of quasielastic helium scattering TOF spectra from $\Theta_{\text{Na}} =$ (a) 0.028 and (b) 0.106 sodium on Cu(001) for different parallel wave vector transfers at a surface temperature of $T_s = 300$ K and an incident beam energy of 11.2 meV along the [100] direction. The experimental points (\odot) show a broadened distribution compared with the instrument response (dashed line). The results of a least-squares fit to the peaks from a convolution of the instrument response with a Lorentz curve are shown by the solid line.

was performed, as outlined in Ref. 30. The substrate–sodium–adatom potential is modeled by a corrugated potential of the form

$$V(x,y) = \frac{E_t}{4} + \frac{E_b}{2} + \frac{E_t}{4} \left[\cos\left(\frac{2\pi x}{a}\right) + \cos\left(\frac{2\pi y}{a}\right) \right] + \frac{1}{4}(E_t - 2E_b) \cos\left(\frac{2\pi x}{a}\right) \cos\left(\frac{2\pi y}{a}\right). \quad (2)$$

The simple cosine potential used previously^{16,18,31} has been modified to allow the top and bridge site diffusion barriers (E_t and E_b) to be varied independently. Here, x and y are displacements parallel to the surface, a is the nearest-neighbor spacing on the substrate surface (2.55 Å), and E_t and E_b are the energies of the on-top site and the bridge site with respect to the fourfold ground-state hollow site. This potential is somewhat different from the two-dimensional potential, denoted V_{GHTCY} , previously obtained by Graham *et al.*^{16,18} as a best fit from a single-adatom Langevin molecular dynamics simulation of the low-coverage diffusion data. The V_{GHTCY} potential was used to explain the observed temperature dependence of the position and width of the T -mode peak. Equation (2) is used here since the number of free parameters is reduced and it is much simpler to calculate while it retains the essential shape of the earlier best-fit potential. The method used here employs the same Langevin equation as in the earlier work^{16,18} to describe the interaction of individual adatoms with the surface. The energy exchange with the substrate was modeled with a Brownian motion type combination of friction, given by the friction parameter η (defined from $dv/dt = -\eta v$) and random impulses to model the transfer of energy from the substrate to the adatoms, as outlined in Ref. 30.

Unlike in the previous simulations for low sodium coverages, the direct repulsive dipole-dipole interaction between the sodium atoms was also taken into account in the present simulations. The sodium-sodium interaction potential was taken to be the Lau and Kohn dipole repulsion potential,²¹

which is twice the interaction of free dipoles due to image charge effects. This potential is described in more detail in the Appendix.

For most of the simulations 512 sodium adatoms were used with a total simulation time of 492 ps (2^{14} time steps) per run, and averages taken over 144 runs. E_t , E_b , and η were varied so as to fit the low-coverage data in both the [100] and $[1\bar{1}0]$ directions over the temperature range 200–300 K. The best fit was obtained for values of the top site barrier of $E_t = 87.5$ meV, a bridge (saddle) site barrier of $E_b = 70$ meV, and friction coefficient $\eta = 0.68$ ps⁻¹. These results are in reasonable agreement with the corresponding values of $E_t = 84$ and $E_b = 75$ eV for V_{GHTCY} , which has a somewhat larger value of $\eta = 0.9$ ps⁻¹. The greater value for η correlates with the 5 meV higher bridge site barrier energy of V_{GHTCY} than in the present case. In order to increase the jump rate to fit the experiment, a higher value of η is therefore required. The best-fit value for $\eta = 0.68$ ps⁻¹ lies between the values of 0.63 ps⁻¹ (220 K) and 0.80 ps⁻¹ (300 K) calculated from the dynamics of a single sodium adatom on a moving slab substrate.¹⁷ Since only phonon-mediated energy transfer between substrate and adsorbate was included in the full simulations, whereas in the current simulations η was varied to fit the data, the rather close agreement between the values obtained suggests that the contribution of the electronic coupling to the friction is relatively small compared to the phonon contribution. The variation of η with temperature predicted by the earlier moving substrate simulations¹⁷ was not included in the current work since it was found to have only a minor effect on the values of E_t and E_b required to fit the data.

V. DISCUSSION OF EXPERIMENTAL AND MOLECULAR DYNAMICS RESULTS

The experimental momentum transfer dependence of the quasielastic broadening is compared with the MD simulations in Fig. 5 for three different temperatures and four different coverages. In the experimental data three important

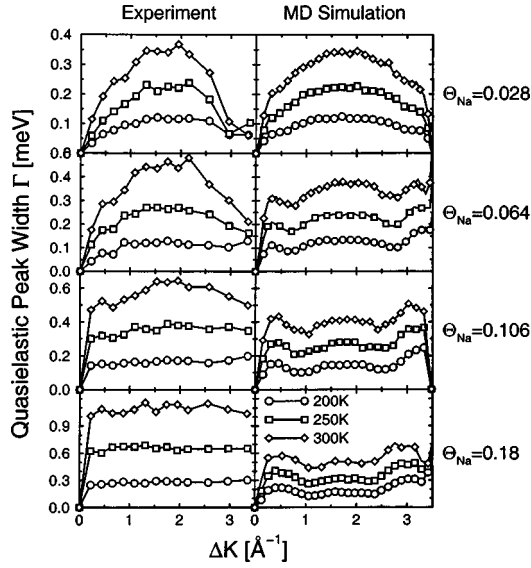


FIG. 5. Comparison of the experimental and MD simulated widths of the quasielastic peak, Γ , as a function of the parallel wave vector transfer ΔK at $T_s = 200, 250,$ and 300 K along the Cu(001) [100] direction for four different sodium coverages Θ_{Na} . The incident beam energy was 11.2 meV.

changes in the $\Gamma(\Delta \mathbf{K})$ curves are observed with increasing coverage. The first is the increase in the effective activation barrier shown in Figs. 2 and 3, the second is a change in the shape of the curve (the broadening rises to its maximum value more quickly as the coverage increases), and the third is that the broadening at the maximum increases as a function of coverage. Each of these coverage-induced changes will now be considered in turn.

A. The coverage dependence of the activation energy

A comparison of the experimental activation energy, as determined from the temperature dependence of the quasielastic broadening at a momentum transfer of 0.86 \AA^{-1} , with the MD simulations is shown in Fig. 3. As can be seen, the experimental value of E_{act} increases from $E_{\text{act}} = 52.5 \pm 0.9$ meV at a low coverage of $\Theta_{\text{Na}} = 0.028$ to $E_{\text{act}} = 63.9 \pm 1.8$ meV for $\Theta_{\text{Na}} = 0.18$. The value of E_{act} at the lower coverages is in excellent agreement with the value of $E_{\text{act}} = 51 \pm 6$ meV determined for $T_s = 175\text{--}400$ K at a coverage of $\Theta_{\text{Na}} = 0.05$.¹³ The activation energies measured here are comparatively low for surface diffusion,¹ and result in a fast rate of diffusion: the mean jump rate for the sodium adatoms at low coverages is 0.13 THz, whereas the frequency of the frustrated translation mode of the Na adatoms is only 1.4 THz. The increase in activation energy shown by the MD simulations is in good agreement with the experiments. This increase in activation energy is attributed to the $1/r^3$ dipole-dipole repulsive interaction between adatoms. Since this potential has a positive second derivative, finite steps toward nearest neighbors increase the activation energy by more than the decrease resulting from steps of the same size but directed away from neighboring atoms, so a step away from some “mean” position will experience a higher activation

energy than a corresponding step made by an isolated adatom that does not experience adatom-adatom interactive forces. This effect can also be simply modeled by arranging six nearest neighbors symmetrically around a central atom, at a distance commensurate with the adatom coverage, and calculating the resulting change in activation energy. The effect on the activation energy is estimated by comparing the energy of the central atom in its initial central position with its energy when it is displaced by half an atomic jump away from this position. The change in activation energy is then averaged over the possible orientations of the hexagon of nearest neighbors with respect to the jump vector. The results of this model are shown by the dashed curve in Fig. 3. The good agreement of both this simple model and the present MD simulations with the data gives strong support for the Lau and Kohn model for the dipole-dipole interaction energy, with twice the free dipole-dipole interaction energy, and a sodium adatom dipole moment strength determined from work function measurements. This suggests that other possible contributions to the adatom-adatom interaction potential are small by comparison.

B. The shape of the broadening curve

At the lowest coverages the interactions between adatoms are weak and, therefore, as outlined in Ref. 30 the Vineyard convolution approximation³² can be used to discuss the $\Gamma(\Delta \mathbf{K})$ curves in terms of simple algebraic models. As outlined in more detail in Ref. 13, a simple jump diffusion model will have a peak width behavior given by

$$\Gamma(\Delta \mathbf{K}) = 2\hbar \sum_{\mathbf{j}} \nu_{\mathbf{j}} [1 - \cos(\mathbf{K} \cdot \mathbf{j})], \quad (3)$$

where $\nu_{\mathbf{j}}$ are the jump frequencies corresponding to jump vectors \mathbf{j} . Thus, if single-jump diffusion occurs between neighboring four-fold hollow sites, then one would expect the broadening curve to be a displaced sinusoidal curve with zeros at $\Delta K = 0$ and 3.48 \AA^{-1} in the [100] direction. The experimental data at the lowest coverage (0.028) do show a pronounced minimum at $\Delta K = 3.48 \text{ \AA}^{-1}$, characteristic of jump diffusion to nearest-neighbor sites. The dip is even more pronounced than in the previously published data^{13,17} because of the better experimental resolution in the current work. The $\Gamma(\Delta \mathbf{K})$ curves for this coverage rise more steeply than they would for a simple displaced sinusoidal curve, indicating the presence of double and possibly longer jumps.^{13,16} The importance of single and double jumps is also seen in the present MD simulations of the system and there is good agreement between the experimental and simulated broadening at $\Theta_{\text{Na}} = 0.028$ (see Fig. 5).

At coverages greater than $\Theta_{\text{Na}} = 0.028$ both the experimental data and the simulations show that the $\Gamma(\Delta \mathbf{K})$ curves rise more rapidly with $\Delta \mathbf{K}$ than is predicted by Eq. (3), suggesting that there is an increasing proportion of longer jump lengths. Moreover, as the interactions between the adatoms become stronger, the interference of the scattering amplitudes from correlated motions of the neighboring atoms, which is neglected in the Vineyard approximation, must be

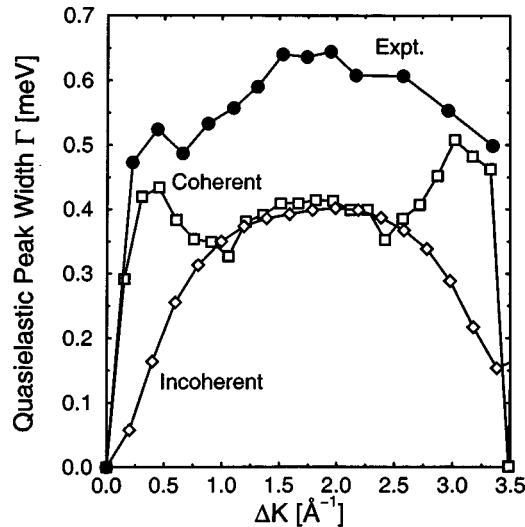


FIG. 6. A comparison between the measured QHAS peak widths (filled circles) and the peak widths derived from the present MD simulations using the coherently scattered intensity (squares), and the widths from a MD simulation of the incoherently scattered intensity only (diamonds). The coverage of sodium was $\Theta_{\text{Na}} = 0.106$, the surface temperature was 300 K, and the incident beam energy was 11.2 meV.

taken into account. Since at very low coverages the sodium atom motions are not appreciably correlated, these interference terms sum to zero but, at higher coverages, as a result of the mutual interactions, the motions become correlated and the interference term can make contributions.

In order to differentiate between the effect of interference and the motion of the individual adatoms, the scattering calculations were also performed *incoherently* by adding the scattering intensities from the individual atoms instead of the amplitudes, so that interference is not included. This is equivalent to using the Vineyard approximation to calculate the quasielastic broadening.³² A comparison between the coherent (true) and incoherent (Vineyard) peak widths is shown in Fig. 6 for a coverage of $\Theta_{\text{Na}} = 0.106$ and a surface temperature of 300 K. It is interesting to see that the shape of the incoherent broadening curve is very similar to that of the coherent one (Fig. 5) at the lowest coverage ($\Theta_{\text{Na}} = 0.028$), indicating that the jump length distribution at a coverage of $\Theta_{\text{Na}} = 0.106$ is similar to that found at the lowest coverage. The more rapid rise in the experimental curves with coverage therefore appears to be due to correlated motions of the sodium adatoms and not due to an enhancement of the long-length jumps.

In Fig. 6 it is interesting to note that in the region $0.75 < \Delta K < 2.6 \text{ \AA}^{-1}$ the coherent and incoherent curves are very similar in form and magnitude, suggesting that the Vineyard approximation is valid for these wave vector transfers. Since these correspond to short distances, mostly to nearest-neighbor sites, the direct influence of correlated motion on the quasielastic broadening is expected to be small. The broadening in this range is, therefore, mainly determined by the jump rate of individual atoms and, although the presence of the neighboring atoms may change this rate, the broaden-

ing here is not significantly affected by the relative times at which an atom and its neighbors jump. Since the mean atomic spacing for $\Theta_{\text{Na}} = 0.106$, corresponding to the peak width curves in Fig. 6, is 8.4 \AA , correlated jumps are expected to occur for wave vectors less than the reciprocal of this distance, i.e., $2\pi/8.4 = 0.75 \text{ \AA}^{-1}$, as well as in the symmetry-related region of K space between $\Delta K = 2.7$ and 4.3 \AA^{-1} around the diffraction peak at $\Delta K = 3.48 \text{ \AA}^{-1}$. It is exactly in these regions that a large increase in quasielastic broadening is seen (Fig. 6).

C. The magnitude of the QE peak width

The maximum value of the experimental peak widths is found to increase roughly by a factor of 3 as the coverage is increased sixfold from 0.028 to 0.18 (Fig. 5). As discussed above, the quasielastic peak widths near the maximum are largely determined by the motion of individual atoms, rather than by the relative timings of jumps made by neighboring atoms. Thus, it may be concluded that the jump rate of the individual Na atoms also increases by a factor of 3 as the coverage rises from 0.028 to 0.18. The MD simulations, however, based on the interaction parameters (friction and potential surface) required to fit the low-coverage QHAS data and the Lau and Kohn Na-Na interaction potential, predict a much smaller 32% increase in QHAS broadening and associated Na atom jump rate. The observed increase in sodium adatom jump rate must be due either to changes in the interactions between the adatoms and the substrate, or to adatom-adatom interactions not accounted for by the Lau and Kohn potential, or the increase is spurious, arising from a peculiar helium-surface scattering effect. We will show, however, that none of these three options can explain the observed increase in jump rate: so much data on this system can be derived from HAS and QHAS measurements that we have been able to test all the possible explanations for the increase that are consistent with the currently accepted understanding of the processes involved in diffusion and collective motion. Clearly some unexpected phenomenon associated with the interrelation of adatom-adatom interactions and diffusion is occurring.

We now consider in turn the possible causes of the observed increase in the adatom jump rate.

(i) The first possible cause is that the friction coefficient η changes with coverage. As was outlined in Ref. 13 and shown by Kramers,^{33,34} the preexponential factor for activated surface diffusion is controlled by the rate of energy transfer between the adatom and the substrate, expressed in terms of η . This rate of energy transfer also determines the intrinsic width of the frustrated translation vibration mode, labeled T in the inset to Fig. 1, and so the FWHM of the T mode was also measured as a function of sodium coverage and temperature. The results are shown in Fig. 7,²⁰ along with a fitted temperature dependence of the T -mode width produced by quadratically adding the intrinsic width (Γ_0), determined by the rate of energy exchange between an adatom and its surroundings, and a linear term ($\propto T$) arising from anharmonic broadening:

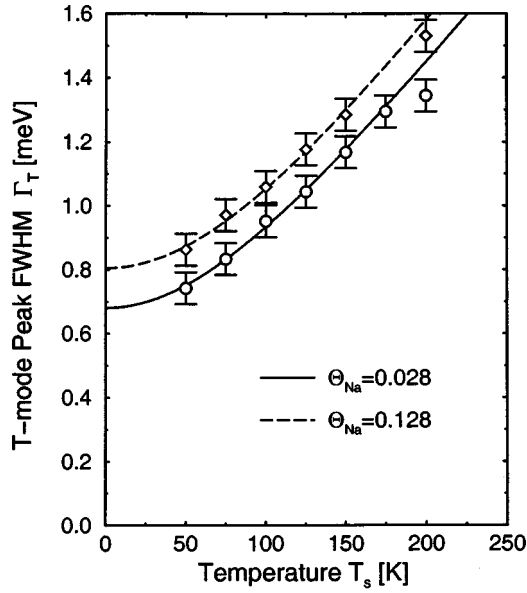


FIG. 7. Temperature dependence of the FWHM of the experimental frustrated translation (T -mode) peak for Na/Cu(001) obtained from TOF measurements of sodium coverages of $\Theta_{\text{Na}} = 0.028$ and 0.128 . The incident energy was $E_i = 20$ meV and the parallel momentum transfer was $\Delta K = 2.0 \text{ \AA}^{-1}$. The curves represent fits to the data that are discussed in the text.

$$\Gamma_T = [\Gamma_0^2 + (\alpha T)^2]^{0.5}. \quad (4)$$

The best fits to the experimental data are shown in Fig. 7 and give values of $\Gamma_0 = 0.68$ meV for a coverage $\Theta_{\text{Na}} = 0.028$ and a somewhat larger value of $\Gamma_0 = 0.805$ meV for a coverage $\Theta_{\text{Na}} = 0.128$. These values are a convolution of the true intrinsic Lorentzian broadening Γ_L and the Gaussian experimental broadening Γ_e . Γ_L is given by³⁵

$$\Gamma_L = \frac{(\Gamma_0^2 - \Gamma_e^2)}{\Gamma_0}. \quad (5)$$

From Eq. (5) the approximate intrinsic peak widths are found to be $\Gamma_L = 0.40$ and 0.56 meV for $\Theta_{\text{Na}} = 0.028$ and 0.128 , which correspond to a total friction experienced by the adatoms of 0.61 and 0.85 ps^{-1} , respectively. The value of 0.61 ps^{-1} for $\Theta_{\text{Na}} = 0.028$ is in excellent agreement with the value for the adsorbate-substrate friction $\eta = 0.68 \text{ ps}^{-1}$ derived from the present molecular dynamics simulations by fitting the low-coverage diffusion data, and confirms the validity of these simulations. The 40% increase in the total friction with coverage indicated by the T -mode peak widths is insufficient to explain the increase in broadening of the quasielastic peak. If, at constant coverage, the value of η used in the simulations is increased by the same fraction, the simulated quasielastic broadening increases by only 25%, far short of the experimentally observed 100% increase in broadening between $\Theta_{\text{Na}} = 0.028$ and 0.128 (see Fig. 1). This

suggests that most of the observed increase in quasielastic broadening with coverage cannot, in fact, be attributed to an increase in the friction.³⁶

(ii) A second possible change is an adjustment of the form of the adatom-substrate potential surface. However, in order to explain the increase in quasielastic broadening by this means, a reduction in the activation energy for diffusion would be required, whereas, as illustrated in Fig. 3, experimentally a slight increase is observed as the coverage rises. Moreover, as outlined in Sec. V A above, this increase in the activation energy with increasing sodium coverage can be fully described by the Lau and Kohn repulsive dipolar potential between sodium atoms used in the present MD simulations,²¹ and so further significant changes in the activation energy cannot be justified.

(iii) The third area for possible adjustment is the strength of the sodium-sodium interaction potential. However, we showed above (Sec. V A) that the Lau and Kohn dipole-dipole interaction model²¹ (see the Appendix) gives a good fit to the experimentally observed variation of the activation energy with coverage. This conclusion was checked by an extensive series of MD simulations in which a wide range of empirical adatom-adatom interaction potentials were used, including inverse power law, exponential, oscillating, and many-body potentials. These showed that a noticeable increase in the sodium atom jump rate could be achieved only by using an adatom-adatom interaction potential that was so strong that it induced strong de Gennes narrowing features³⁷ in the simulated $\Gamma(\Delta \mathbf{K})$ curves,³⁰ which are clearly not observed experimentally. Extra terms in the sodium-sodium interaction potential may therefore be ruled out as a cause of the observed increase in sodium adatom jump rate with temperature.

(iv) Yet another way in which the simulations might be modified to reproduce the experimentally observed increase in quasielastic broadening with coverage would be to include the effects of multiple scattering. The kinematic approximation does not include multiple scattering, and it could be proposed that a helium atom scattered from more than one moving surface adatom could pick up an increased quasielastic broadening. This effect would be most significant at higher coverages where the multiple scattering will become more pronounced. True multiple scattering calculations would take prohibitively long, and so a simple extension of the kinematic approximation is used to obtain a rough guide to the magnitude of the possible error. In this simple s -wave scattering model, each atom scatters an incident wave of unit amplitude, which gives rise to a spherical outgoing wave with an intensity of $\sigma/(4\pi r^2)$ at a distance r from the scatterer, where σ is the scattering cross section. The amplitude (f_j) incident upon the j th atom is then given by the sum (with the proper phases) of the amplitude of the incident wave and the scattering amplitudes from the k th neighbors:

$$f_j = e^{i\mathbf{K}_i \cdot \mathbf{R}_j} + \frac{\sqrt{\sigma}}{2\sqrt{\pi}} \sum_k \frac{f_k}{|\mathbf{R}_j - \mathbf{R}_k|} e^{i\mathbf{k}_i \cdot |\mathbf{R}_j - \mathbf{R}_k|}, \quad (6)$$

where \mathbf{K}_i is the surface parallel component of the incident helium wave vector \mathbf{k}_i . This matrix equation was solved for each time step for the f values and the scattered amplitude for this time step was calculated as

$$M(\Delta\mathbf{K}, t) = \sum_{j=1}^N f_j e^{-i\mathbf{K}_f \cdot \mathbf{R}_j}, \quad (7)$$

where \mathbf{K}_f is the component of the outgoing helium wave vector parallel to the surface and M is the time-dependent amplitude function.

The multiple scattering cross section σ was varied from zero to 36 \AA^2 , where the latter value corresponds to the area of surface per adatom in the MD simulations and so represents an upper limit for σ . For $\sigma < 18 \text{ \AA}^2$ no change is observed in the quasielastic broadening. Above this value, the scattering calculations start to break down, with the scattered intensity diverging, indicating an unrealistically high value of the cross section. These simple calculations suggest, therefore, that multiple scattering is also probably not the cause of the discrepancy between the simulations and the experimental data.

Therefore we conclude that none of the above explanations can account for the experimentally observed increase in the quasielastic broadening with coverage.

VI. CONCLUSIONS

Quasielastic helium scattering has been used to extend the previous low-coverage measurements of the microscopic diffusional motion of sodium atoms on a Cu(001) surface^{13,16,18} up to coverages as high as $\Theta_{\text{Na}} = 0.18$, where interactions between the adsorbates are expected to become important. This situation corresponds to a two-dimensional quasiliquid phase. The experimental results are compared with extensive Langevin-type molecular dynamics simulations that account for the interaction between the sodium atoms via the Lau and Kohn dipole-dipole interaction potential and the coupling to the substrate by a corrugated two-dimensional potential and a Brownian motion type combination of friction and random impulses. The most important assumption made in the simulation of the results at higher coverages is that the He atoms scatter only from single adatoms. This was tested by using a simple multiple scattering model which had no appreciable effect on the MD simulation results. Although the present MD simulations were not able to explain the measured three-fold increase in the quasielastic peak width and some other observed features for coverages $\Theta_{\text{Na}} > 0.064$, a number of important conclusions may be drawn. The energy exchange between the adatoms and the substrate could be quantified, leading to a value for the friction of $\eta = 0.63 \text{ ps}^{-1}$ in good agreement with earlier work.¹³ The experimentally observed increase in the activation energy with coverage is well reproduced by a dipole-dipole interaction potential with twice the free dipole-dipole interaction energy and an adatom dipole moment determined from work function measurements, as proposed by Lau and Kohn²¹ (see the Appendix). To the authors' knowledge these measurements represent the first

validation of their formula. At higher coverages the adatom-adatom interactions, while leaving the basic jump length distributions apparently unaffected, could be shown to lead to correlations in the motions of the adatoms that change the momentum dependence of the quasielastic broadening. In an effort to explain the large discrepancy in the peak widths, four different possible effects were critically discussed and analyzed, but found to be unable to explain the results. The comprehensive body of data represented here will make possible a rigorous test of any future explanation of this dramatic but enigmatic effect.

ACKNOWLEDGMENTS

The authors would like to thank Professor S. C. Ying for many helpful discussions during the preparation of this manuscript. J.E. would like to thank the Lloyd's of London Tercentenary Foundation for financial support that enabled him to carry out the simulations reported in this paper.

APPENDIX

When sodium is adsorbed on the Cu(001) surface, a diffuse ring of elastic intensity is observed around the specular peak.^{19,38} The diameter of this ring increases roughly with the square root of the coverage. The ring forms because a region of clear surface is created around each adatom by the interadatom repulsion, and the Fourier transform of this hole in the pair distribution function $g(R)$ leads to a ring of intensity around the diffracted peaks. The observed repulsive adatom-adatom interaction potential is generally attributed to the electrostatic repulsion between the dipoles resulting from the transfer of charge from the sodium to the substrate. The magnitude of this interaction was calculated by Lau and Kohn²¹ to be twice the repulsion between free dipoles due to polarization of the substrate electron density by the adsorbate dipole moment leading to an image dipole of the same magnitude. The summation of the adsorbate and image dipole moments provides the factor of 2.²¹ The dipole moment of the adsorbate alone can be extracted from work function change ($\Delta\phi$) measurements²³ using the Topping model of the coverage-dependent dipole-induced depolarization:³⁹

$$\Delta\phi = \frac{p_0 n_0 \Theta_{\text{Na}}}{\epsilon_0 [1 + 9\alpha(n_0 \Theta_{\text{Na}})^{1.5}]}, \quad (\text{A1})$$

where n_0 is the adatom density at a coverage of $\Theta_{\text{Na}} = 1$. The experimental work function changes were fitted by values for p_0 , the low-coverage limit for the sodium dipole moment, of $0.58 \text{ \AA} e$ (e is the charge on an electron) and for α , the polarizability of the sodium adatoms, 17.7 \AA^3 .²³ These values can then be used to calculate the mean adatom dipole moment at a particular coverage given by

$$p_{\text{mean}} = \frac{p_0}{1 + 9\alpha(n_0 \Theta_{\text{Na}})^{1.5}}. \quad (\text{A2})$$

This dipole moment is used to calculate the interadatom interaction potential in the simulations.

- ¹R. Gomer, Rep. Prog. Phys. **53**, 917 (1990).
- ²G. Ehrlich, Surf. Sci. **299/300**, 628 (1994).
- ³M. C. Tringides, Surf. Sci. **204**, 345 (1988).
- ⁴X. D. Xiao, Y. Xie, and Y. R. Shen, Surf. Sci. **271**, 295 (1992).
- ⁵X. D. Zhu, T. Rasing, and Y. R. Shen, Phys. Rev. Lett. **61**, 2883 (1988).
- ⁶W. Zhao, R. W. Verhoef, and M. Asscher, J. Chem. Phys. **107**, 5554 (1997).
- ⁷B. S. Swartzentruber, Phys. Rev. Lett. **76**, 459 (1996); T. Zambelli, J. Trost, J. Winterlin, and G. Ertl, *ibid.* **76**, 795 (1996).
- ⁸J. W. M. Frenken and B. J. Hinch, in *Quasielastic Helium Scattering Studies of Adatom Diffusion on Surfaces*, Vol. 27 of Springer Series in Surface Sciences, edited by E. Hulpke (Springer-Verlag, Berlin, 1992), p. 287.
- ⁹M. Bée, Quasielastic Neutron Scattering (Adam Hilger, Bristol, 1988).
- ¹⁰J. W. M. Frenken, B. J. Hinch, and J. P. Toennies, Surf. Sci. **211/212**, 21 (1989).
- ¹¹J. W. M. Frenken, B. J. Hinch, J. P. Toennies, and Ch. Wöll, Phys. Rev. B **41**, 938 (1990).
- ¹²B. J. Hinch, J. W. M. Frenken, G. Zhang, and J. P. Toennies, Surf. Sci. **259**, 288 (1992).
- ¹³J. Ellis and J. P. Toennies, Phys. Rev. Lett. **70**, 2118 (1993).
- ¹⁴A. P. Graham, W. Silvestri, and J. P. Toennies, in *Surface Diffusion: Atomistic and Collective Processes*, Vol. 360 of NATO Advanced Study Institute, Series B: Physics, edited by M. Tringides (Plenum, New York, 1997), p. 565.
- ¹⁵A. P. Graham and J. P. Toennies, Surf. Sci. **427-8**, 1 (1999).
- ¹⁶A. P. Graham, F. Hofmann, J. P. Toennies, L. Y. Chen, and S. C. Ying, Phys. Rev. Lett. **78**, 3900 (1997).
- ¹⁷J. Ellis and J. P. Toennies, Surf. Sci. **317**, 99 (1994).
- ¹⁸A. P. Graham, F. Hofmann, J. P. Toennies, L. Y. Chen, and S. C. Ying, Phys. Rev. B **56**, 10 567 (1997).
- ¹⁹A. P. Graham and J. P. Toennies, Phys. Rev. B **56**, 15 390 (1997).
- ²⁰P. Senet, A. P. Graham, J. P. Toennies, and G. Witte (unpublished).
- ²¹K. H. Lau and W. Kohn, Solid State Commun. **18**, 553 (1976).
- ²²G. Witte, Ph.D. thesis, Max-Planck-Institut für Strömungsforschung, Göttingen, Germany, 1995.
- ²³A. Cucchetti and S. C. Ying, Phys. Rev. B **60**, 11 110 (1999).
- ²⁴J. P. Toennies, in *Surface Phonons*, Vol. 14 of *Springer Series in Surface Sciences*, edited by F. de Wette (Springer-Verlag, Berlin, 1988), p. 248.
- ²⁵F. Hofmann, J. R. Manson, and J. P. Toennies, J. Chem. Phys. **101**, 10 155 (1994).
- ²⁶Sodium dispenser NA/NF/2.2/12 from SAES Getters S.p.A., Via Gallarate 215, I-20151 Milano, Italy.
- ²⁷B. Poelsema and G. Comsa, *Scattering of Thermal Energy Atoms from Disordered Surfaces*, Vol. 115 of *Springer Tracts in Modern Physics* (Springer-Verlag Berlin, 1989).
- ²⁸G. Benedek, J. Ellis, N. S. Luo, A. Reichmuth, P. Ruggerone, and J. P. Toennies, Phys. Rev. B **48**, 4917 (1993).
- ²⁹F. Hofmann, W. Schöllkopf, and J. P. Toennies, *Proceedings of the Welch Foundation, Conference on Chemical Research, Chemical Dynamics of Transient Species Houston, 1994* (The Robert H. Welch Foundation, Houston, 1994).
- ³⁰J. Ellis and A. P. Graham, Surf. Sci. **377-379**, 833 (1997).
- ³¹L. Y. Chen and S. C. Ying, Phys. Rev. Lett. **71**, 4361 (1993).
- ³²G. H. Vineyard, Phys. Rev. **110**, 999 (1958).
- ³³H. A. Kramers, Physica (Amsterdam) **7**, 285 (1940).
- ³⁴P. Hänggi, P. Talkner, and M. Borkovec, Rev. Mod. Phys. **62**, 251 (1990).
- ³⁵A. P. Graham and J. P. Toennies, Europhys. Lett. **42**, 449 (1998).
- ³⁶Simulations that incorporated a position-dependent friction failed to induce a noticeable change in the $\Gamma(\Delta\mathbf{K})$ curves.
- ³⁷P. G. De Gennes, Physica (Amsterdam) **25**, 825 (1959).
- ³⁸F. Hofmann, Ph.D. thesis, Max Planck Institut für Strömungsforschung, Göttingen, Germany, 1996.
- ³⁹J. Topping, Proc. R. Soc. London, Ser. A **114**, 67 (1927); A. R. Miller, Proc. Cambridge Philos. Soc. **42**, 292 (1946).